Figure S1

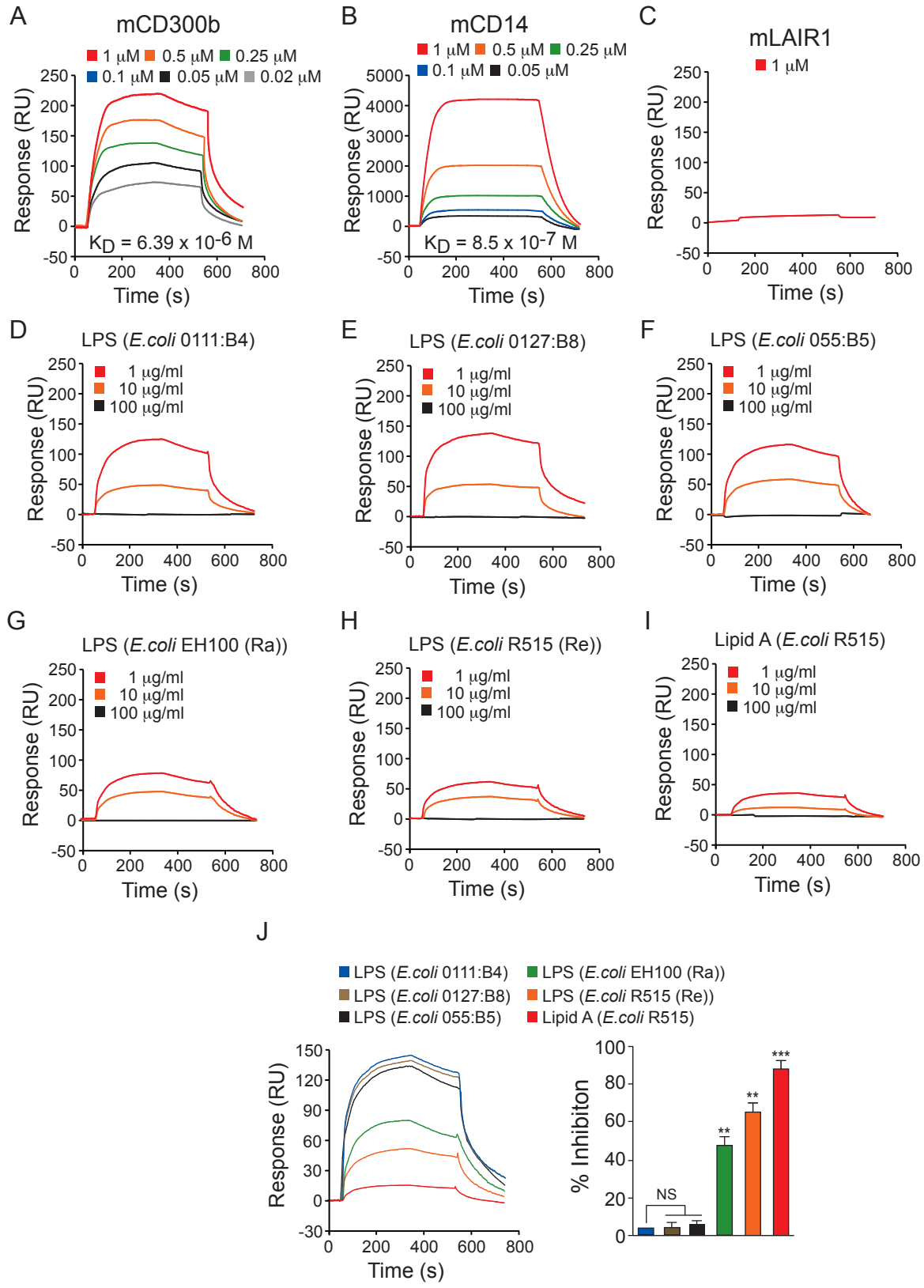
A
mCD300b
1 μM 0.5 μM 0.25 μM
0.1 μM 0.05 μM 0.02 μM
Response (RU)
Time (s)
KD = 6.39 x 10-6 M
B
mCD14
1 μM 0.5 μM 0.25 μM
0.1 μM 0.05 μM
Response (RU)
Time (s)
KD = 8.5 x 10-7 M
C
mLAIR1
1 μM
Response (RU)
Time (s)
D
LPS (E.coli 0111:B4)
1 μg/ml
10 μg/ml
100 μg/ml
Response (RU)
Time (s)
E
LPS (E.coli 0127:B8)
1 μg/ml
10 μg/ml
100 μg/ml
Response (RU)
Time (s)
F
LPS (E.coli 055:B5)
1 μg/ml
10 μg/ml
100 μg/ml
Response (RU)
Time (s)
G
LPS (E.coli EH100 (Ra))
1 μg/ml
10 μg/ml
100 μg/ml
Response (RU)
Time (s)
H
LPS (E.coli R515 (Re))
1 μg/ml
10 μg/ml
100 μg/ml
Response (RU)
Time (s)
I
Lipid A (E.coli R515)
1 μg/ml
10 μg/ml
100 μg/ml
Response (RU)
Time (s)
J
LPS (E.coli 0111:B4)
LPS (E.coli EH100 (Ra))
LPS (E.coli 0127:B8)
LPS (E.coli R515 (Re))
LPS (E.coli 055:B5)
Lipid A (E.coli R515)
Response (RU)
Time (s)
% Inhibiton
NS
**
**
***

Figure S2

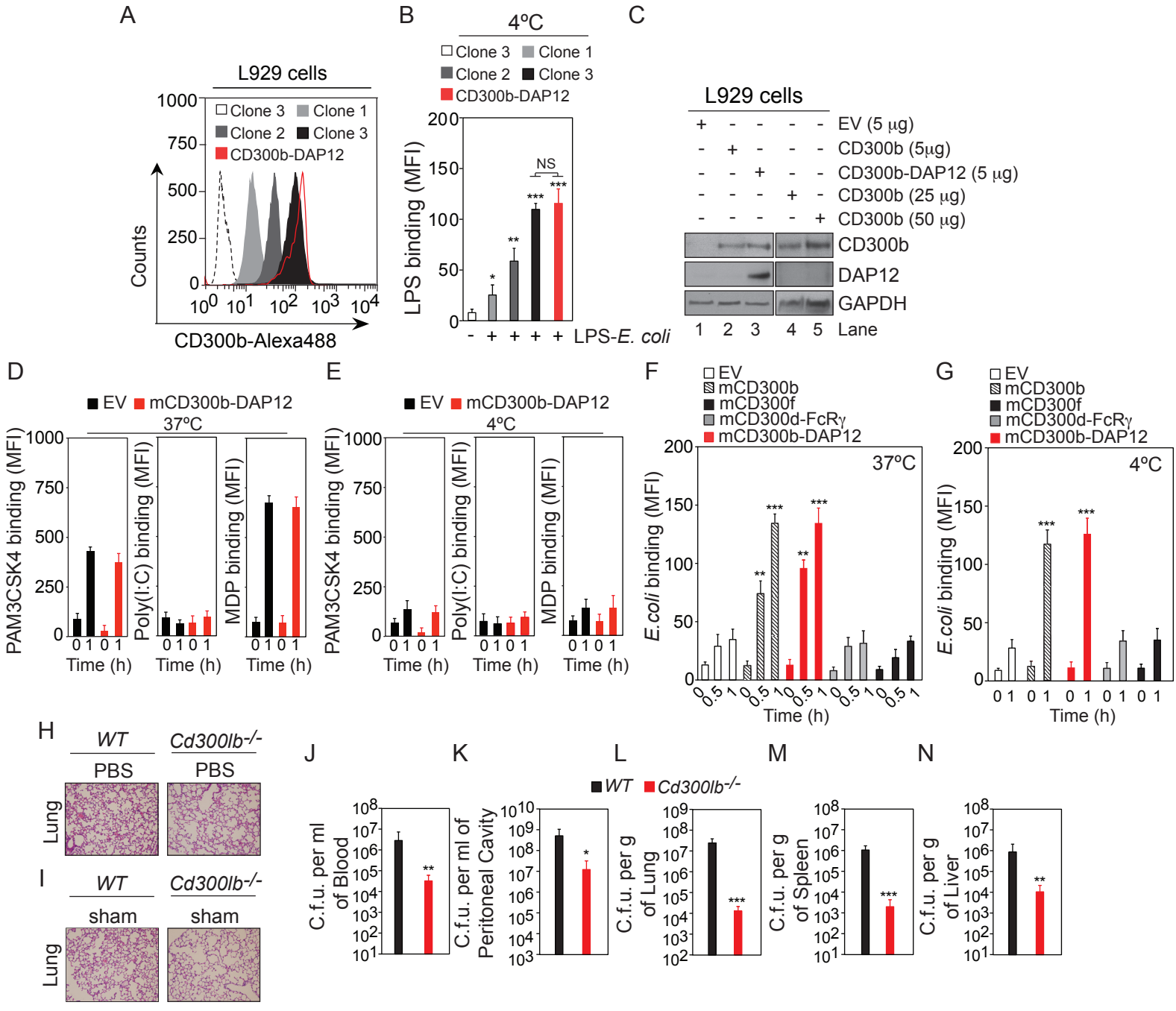
A
L929 cells
Clone 3
Clone 1
Clone 2
Clone 3
CD300b-DAP12
Counts
CD300b-Alexa488
B
4ºC
Clone 3
Clone 1
Clone 2
Clone 3
CD300b-DAP12
LPS binding (MFI)
NS
LPS-E. coli
C
L929 cells
EV (5 μg)
CD300b (5μg)
CD300b-DAP12 (5 μg)
CD300b (25 μg)
CD300b (50 μg)
CD300b
DAP12
GAPDH
Lane
D
EV
mCD300b-DAP12
37ºC
PAM3CSK4 binding (MFI)
Poly(I:C) binding (MFI)
MDP binding (MFI)
Time (h)
E
EV
mCD300b-DAP12
4ºC
PAM3CSK4 binding (MFI)
Poly(I:C) binding (MFI)
MDP binding (MFI)
Time (h)
F
EV
mCD300b
mCD300f
mCD300d-FcRγ
mCD300b-DAP12
37ºC
E.coli binding (MFI)
Time (h)
G
EV
mCD300b
mCD300f
mCD300d-FcRγ
mCD300b-DAP12
4ºC
E.coli binding (MFI)
Time (h)
H
WT
Cd300lb-/-
PBS
PBS
Lung
I
WT
Cd300lb-/-
sham
sham
Lung
J
C.f.u. per ml of Blood
K
C.f.u. per ml of Peritoneal Cavity
L
WT
Cd300lb-/-
C.f.u. per g of Lung
M
C.f.u. per g of Spleen
N
C.f.u. per g of Liver

Figure S3

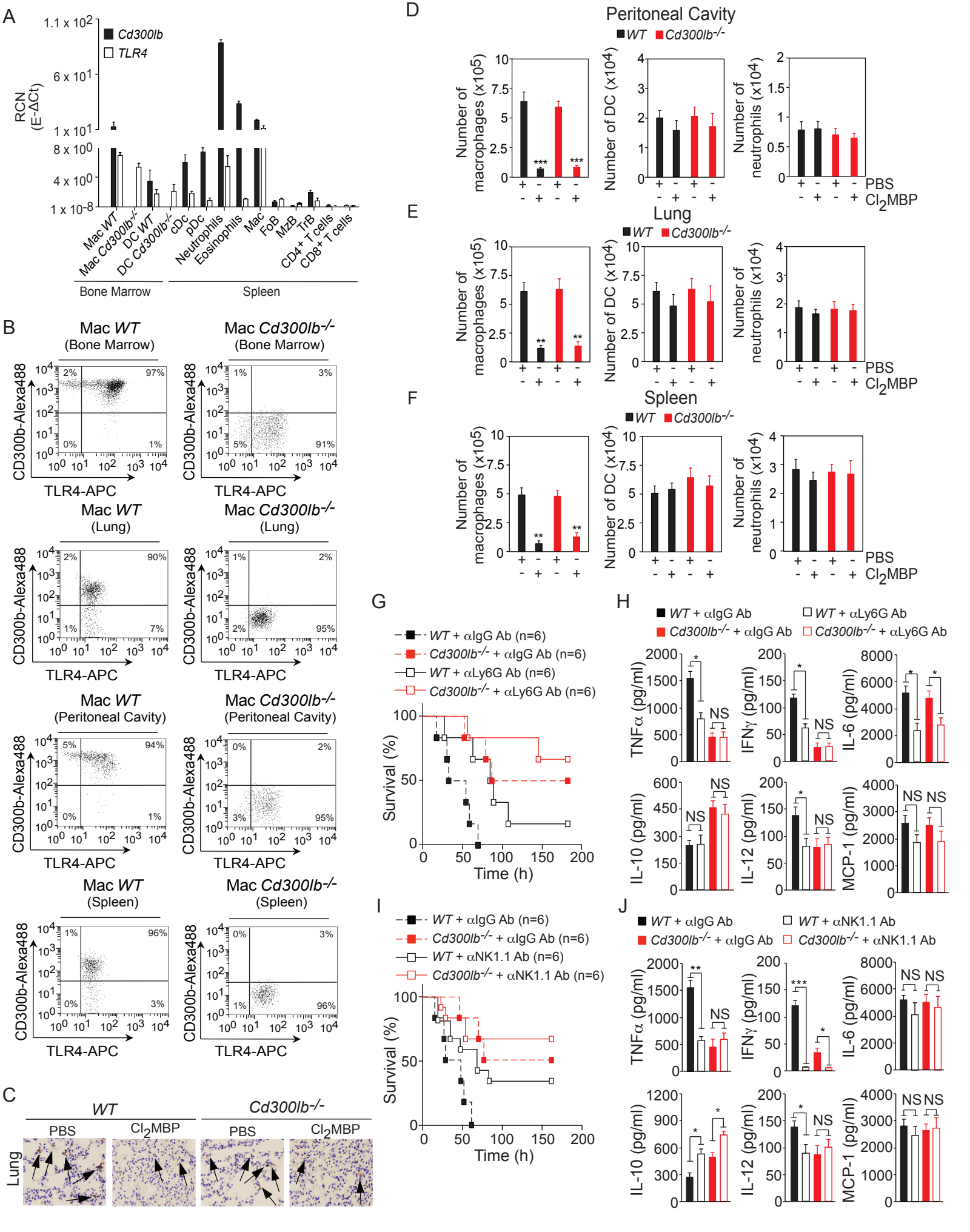
A
Cd300lb
TLR4
RCN (E-ΔCt)
Mac WT
Mac Cd300lb-/-
DC WT
DC Cd300lb-/-
cDc
pDc
Neutrophils
Eosinophils
Mac
FoB
MzB
TrB
CD4+ T cells
CD8+ T cells
Bone Marrow
Spleen
B
Mac WT (Bone Marrow)
Mac Cd300lb-/- (Bone Marrow)
Mac WT (Lung)
Mac Cd300lb-/- (Lung)
Mac WT (Peritoneal Cavity)
Mac Cd300lb-/- (Peritoneal Cavity)
Mac WT (Spleen)
Mac Cd300lb-/- (Spleen)
CD300b-Alexa488
TLR4-APC
C
WT
Cd300lb-/-
PBS
Cl2MBP
Lung
D
Peritoneal Cavity
WT
Cd300lb-/-
Number of macrophages (x105)
Number of DC (x104)
Number of neutrophils (x104)
PBS
Cl2MBP
E
Lung
F
Spleen
G
WT + αIgG Ab (n=6)
Cd300lb-/- + αIgG Ab (n=6)
WT + αLy6G Ab (n=6)
Cd300lb-/- + αLy6G Ab (n=6)
Survival (%)
Time (h)
H
WT + αIgG Ab
WT + αLy6G Ab
Cd300lb-/- + αIgG Ab
Cd300lb-/- + αLy6G Ab
TNFα (pg/ml)
IFNγ (pg/ml)
IL-6 (pg/ml)
IL-10 (pg/ml)
IL-12 (pg/ml)
MCP-1 (pg/ml)
NS
I
WT + αIgG Ab (n=6)
Cd300lb-/- + αIgG Ab (n=6)
WT + αNK1.1 Ab (n=6)
Cd300lb-/- + αNK1.1 Ab (n=6)
Survival (%)
Time (h)
J
WT + αIgG Ab
WT + αNK1.1 Ab
Cd300lb-/- + αIgG Ab
Cd300lb-/- + αNK1.1 Ab
TNFα (pg/ml)
IFNγ (pg/ml)
IL-6 (pg/ml)
IL-10 (pg/ml)
IL-12 (pg/ml)
MCP-1 (pg/ml)
NS

Figure S4

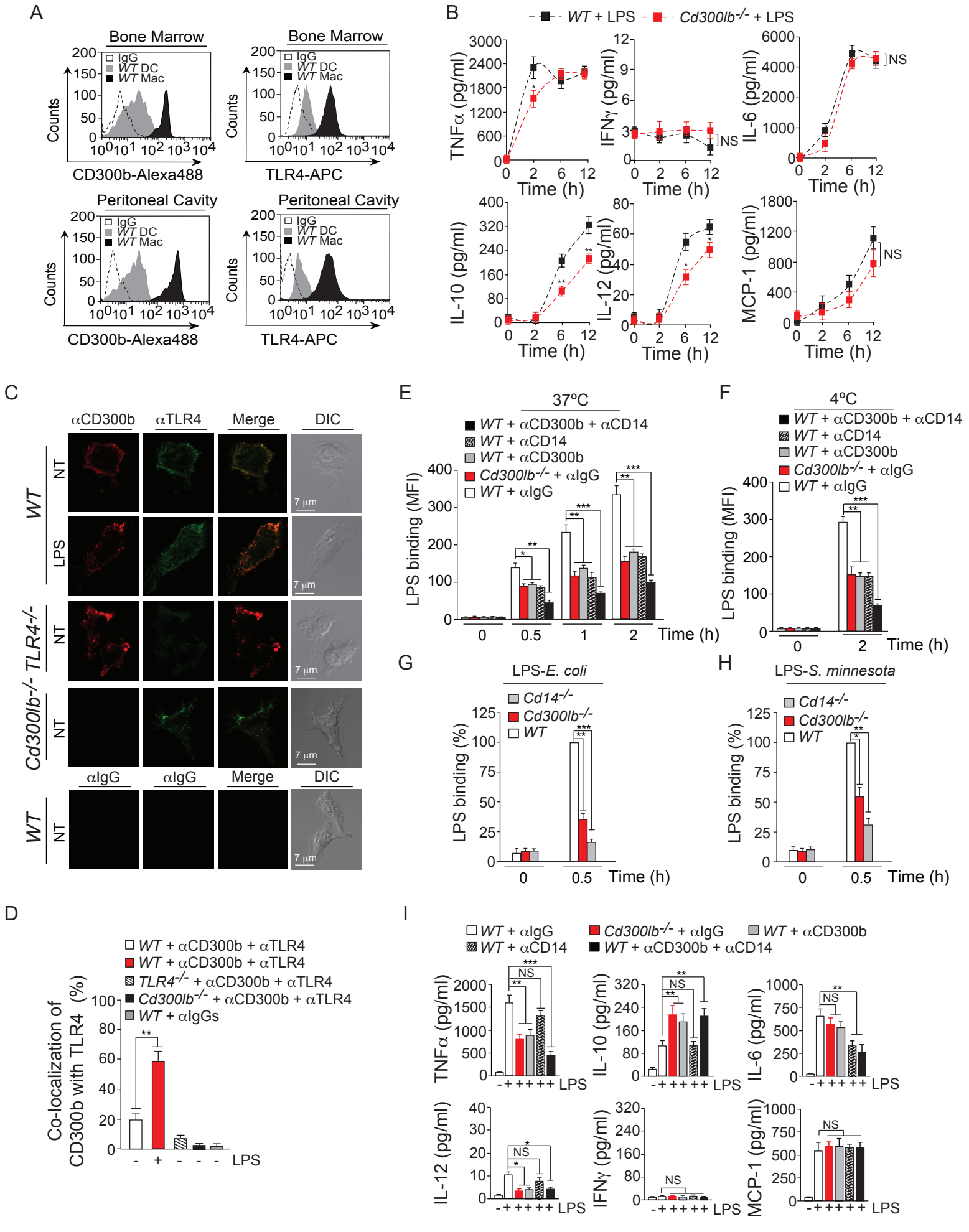
A
Bone Marrow
Peritoneal Cavity
IgG
WT DC
WT Mac
Counts
CD300b-Alexa488
TLR4-APC
B
WT + LPS
Cd300lb-/- + LPS
TNFα (pg/ml)
IFNγ (pg/ml)
IL-6 (pg/ml)
IL-10 (pg/ml)
IL-12 (pg/ml)
MCP-1 (pg/ml)
Time (h)
NS
C
αCD300b
αTLR4
Merge
DIC
αIgG
WT
Cd300lb-/-
TLR4-/-
NT
LPS
7 μm
D
WT + αCD300b + αTLR4
TLR4-/- + αCD300b + αTLR4
Cd300lb-/- + αCD300b + αTLR4
WT + αIgGs
Co-localization of CD300b with TLR4 (%)
LPS
E
37°C
WT + αCD300b + αCD14
WT + αCD14
WT + αCD300b
Cd300lb-/- + αIgG
WT + αIgG
LPS binding (MFI)
F
4°C
G
LPS-E. coli
Cd14-/-
Cd300lb-/-
WT
LPS binding (%)
H
LPS-S. minnesota
I
WT + αIgG
WT + αCD14
Cd300lb-/- + αIgG
WT + αCD300b
WT + αCD300b + αCD14

Figure S5

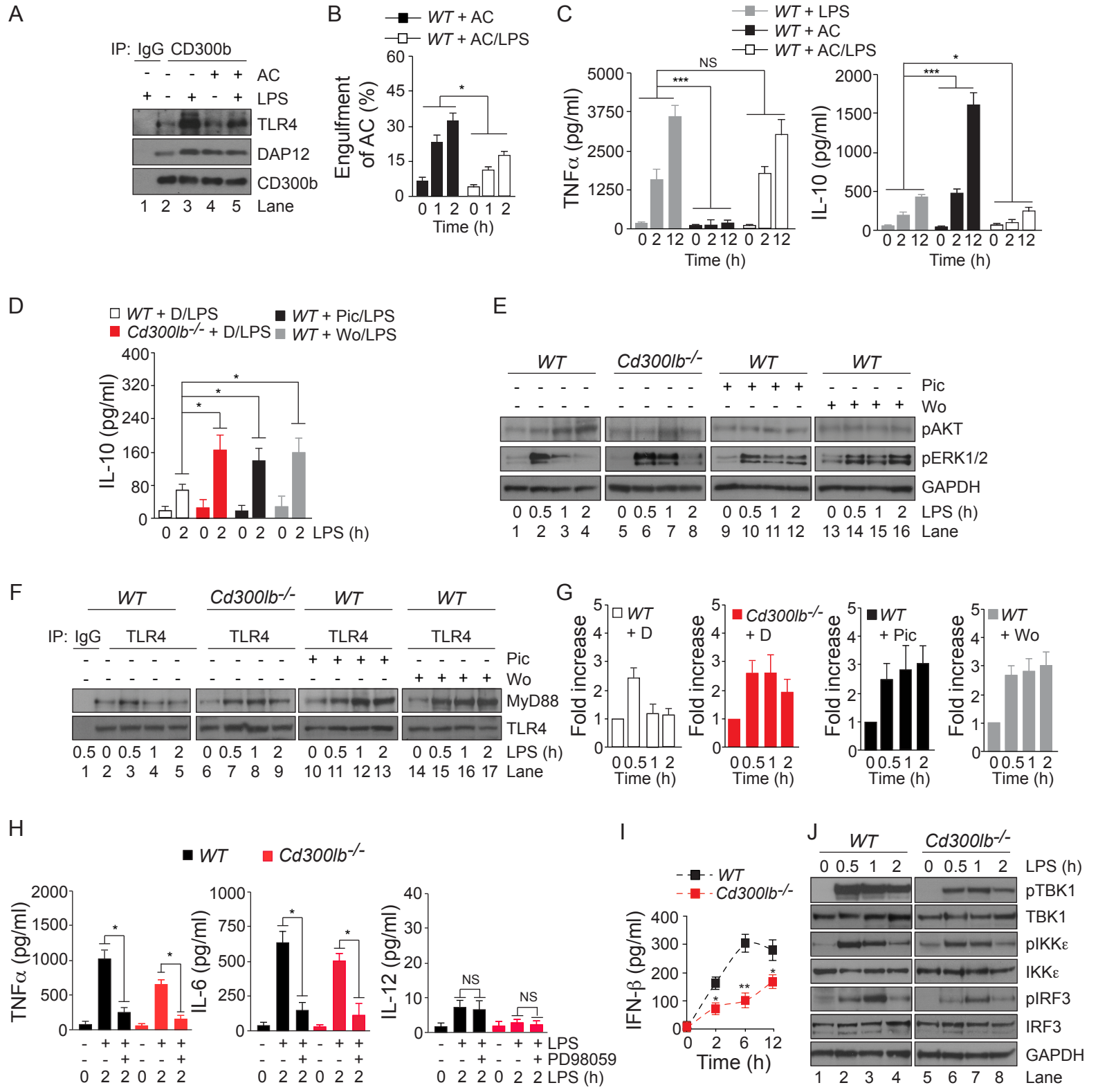
A
IP: IgG CD300b
AC
LPS
TLR4
DAP12
CD300b
1 2 3 4 5 Lane
B
WT + AC
WT + AC/LPS
Engulfment of AC (%)
Time (h)
C
WT + LPS
WT + AC
WT + AC/LPS
NS
TNFα (pg/ml)
IL-10 (pg/ml)
Time (h)
D
WT + D/LPS
Cd300lb-/- + D/LPS
WT + Pic/LPS
WT + Wo/LPS
IL-10 (pg/ml)
LPS (h)
E
WT
Cd300lb-/-
Pic
Wo
pAKT
pERK1/2
GAPDH
LPS (h)
Lane
F
IP: IgG TLR4
MyD88
TLR4
LPS (h)
Lane
G
WT + D
Cd300lb-/- + D
WT + Pic
WT + Wo
Fold increase
Time (h)
H
WT
Cd300lb-/-
TNFα (pg/ml)
IL-6 (pg/ml)
IL-12 (pg/ml)
NS
LPS
PD98059
LPS (h)
I
WT
Cd300lb-/-
IFN-β (pg/ml)
Time (h)
J
WT
Cd300lb-/-
LPS (h)
pTBK1
TBK1
pIKKε
IKKε
pIRF3
IRF3
GAPDH
Lane

Figure S6

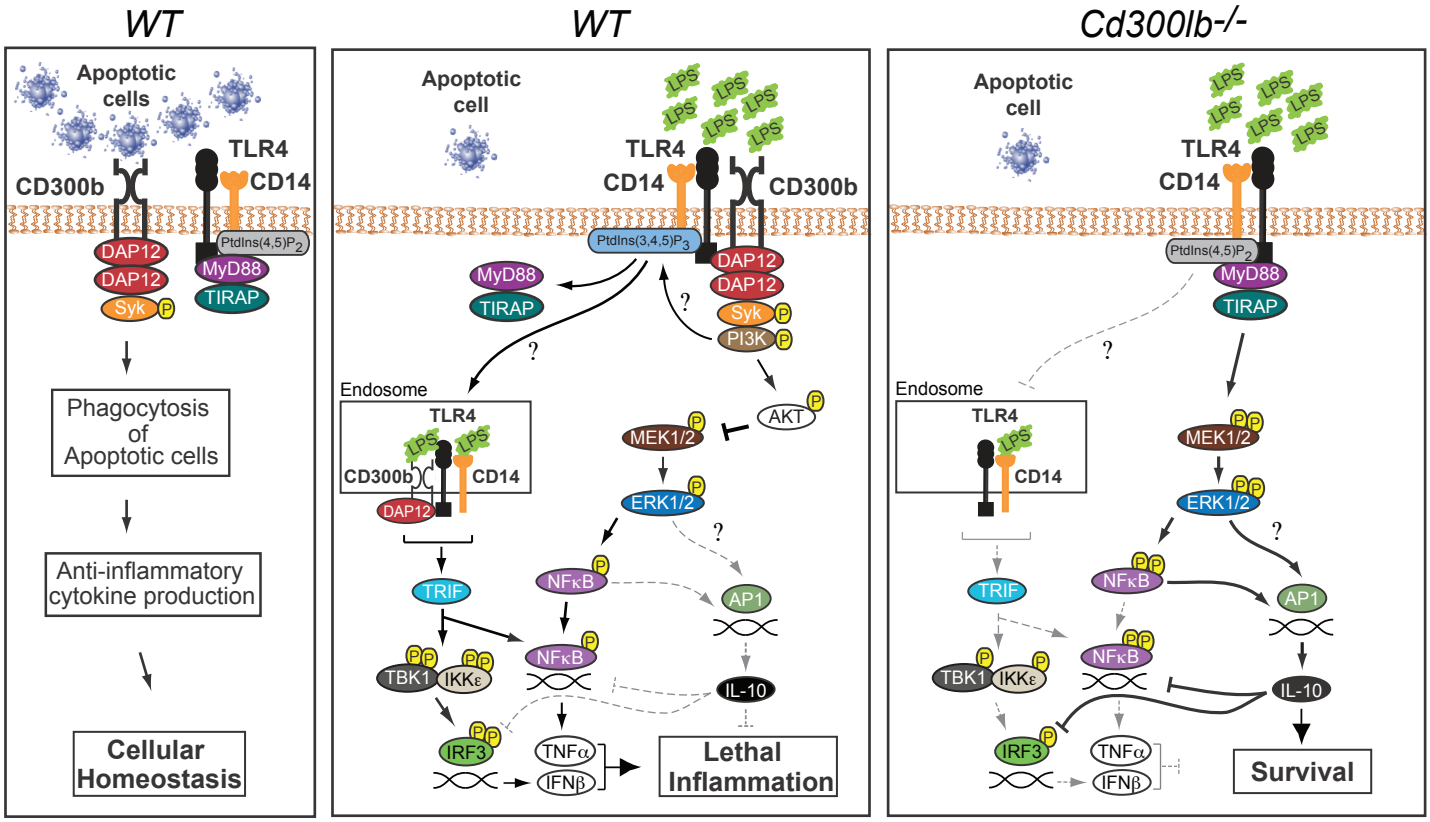
WT
WT
Cd300lb-/-
Apoptotic cells
Apoptotic cell
Apoptotic cell
TLR4
CD14
CD300b
PtdIns(4,5)P2
PtdIns(3,4,5)P3
DAP12
MyD88
TIRAP
Syk
PI3K
LPS
Phagocytosis of Apoptotic cells
Anti-inflammatory cytokine production
Cellular Homeostasis
Endosome
MEK1/2
ERK1/2
AKT
TRIF
NFκB
AP1
TBK1
IKKε
IRF3
TNFα
IFNβ
IL-10
Lethal Inflammation
Survival
Physiological conditions
Acute bacterial infection

Supplementary Figure legends:

Figure S1, related to Figure 1. CD300b recognizes LPS via the lipid A core structure
(A-C) Sensorgrams of mCD300b (A), mCD14 (B), and mLAIR1 (C) protein binding to immobilized LPS (*E.coli* 0111:B4) over the indicated times.
(D-I) Sensorgrams of mCD300b protein binding to immobilized LPS (*E.coli* 0111:B4) after pre-incubation with various wild-type LPS serotypes LPS-*E.coli* (0111:B4; D), LPS-*E.coli* (0127:B8; E), LPS-*E.coli* (055:B5; F), or different LPS structural components: LPS-*E.coli* (EH100 (Ra); G), LPS-*E.coli* (R515 (Re); H), or lipid A-*E.coli* (R515 (Re); I) over the indicated times.
(J) Sensorgram overlays and quantification of mCD300b binding to immobilized LPS after pre-incubation with different wild-type LPS-*E.coli* serotypes (D-F), or various LPS structures (G-I) (1 μg/ml). Binding for all sensorgrams (A-I) was initiated at 60 s and the dissociation phase begun at 240 s and is expressed in resonance units (RU). Data in (A-J) are a representative of three experiments. The graph (J) show mean values + SEM; **p≤0.01, and ***p≤0.001.

Figure S2, related to Figure 1 and 2. CD300b binds LPS or *E. coli* but not other TLR or NOD ligands and CLP-treated *WT* but not *Cd300lb*$^{-/-}$ mice have a higher bacterial burden.
(A-B) mCD300b-DAP12- (MFI: 144) or clonal cell lines expressing different levels of cell surface mCD300b- (Clone 1, MFI: 34; Clone 2, MFI: 86; Clone 3, MFI: 138) were incubated with FITC-labeled LPS from *E. coli* (10 μg/ml) for 1 h at 4°C. Binding was analyzed by flow cytometry and expressed as MFI.
(C) mCD300b-DAP12-, mCD300b- and EV-expressing L929 cells were lysed and the expression level of CD300b and DAP12 (overexpressed and endogenous) was assessed by immunoblotting with the indicated Abs. GAPDH served as loading control.
(D-E) mCD300b-DAP12- and EV-expressing L929 cells were incubated with rhodamine-labeled PAM3CSK4, Poly(I:C) or MDP (10 μg/ml) for 1 h at 37°C (D) or 4°C (E). Binding was analyzed by flow cytometry and displayed as MFI.
(F-G) mCD300b-, mCD300b-DAP12-, mCD300d-FcRγ-, mCD300f- or EV-expressing L929 cells were incubated with FITC-labeled *E. coli* (10 μg/ml) for 0.5 and 1 h at 37°C (F) or 4°C (G). Binding was analyzed by flow cytometry and displayed as MFI.
(H-I) *WT* and *Cd300lb*$^{-/-}$ mice were i.p. injected with PBS (H) or subjected to laparotomy without ligation and puncture (sham-control) (I). Lung tissues were stained using H&E. Tissue sections shown are representative of 5 mice per group.
(J-N) Bacterial burden was determined in *WT* and *Cd300lb*$^{-/-}$ mice 24 h after CLP-treatment. The number of colony formation units (c.f.u.) in the blood (J), peritoneal cavity (K), lung (L), spleen (M) and liver (N) was assessed by plating 10-fold serial dilutions of fluids or homogenized organ tissues. Histograms in (A) and immunoblots shown in (C) are representative of three experiments. The graphs show mean values + SEM from three experiments (B and D-G) or 5 mice (J-N) per group; NS, not significant; *p≤0.05, **p≤0.01, and ***p≤0.001.

Figure S3, related to Figure 4. CD300b-TLR4 co-expressing macrophages were depleted *in vivo* using dichloromethylene biphosphate (Cl_2MBP)-encapsulated liposomes, while selective reduction of CD300b-expressing neutrophils or NK cells does not augment the pathogenesis of lethal endotoxemia.
(A) Quantitative real-time RT-PCR analysis of CD300b and TLR4 expression on immune cells differentiated from the bone marrow or isolated from the spleen from *WT* or *Cd300lb*$^{-/-}$ mice. Selected immune cells isolated from spleen tissue were sorted by flow cytometry using morphological and cell surface specific markers into the following populations: cDC, conventional dendritic cells ($CD11c^{hi}$ $B220^{-}$); pDC, plasmacytoid DC ($CD11c^{lo}B220^{+}$PDCA-1^{+}); Mac, macrophages ($CD11b^{hi}CD11c^{-}Ly6G^{-}SSC^{lo}$); eosinophils ($CD11b^{hi}CD11c^{-}Ly6G^{lo}SSC^{hi}$); neutrophils ($CD11b^{hi}CD11c^{-}Ly6G^{hi}SSC^{lo}$); FoB, follicular B cells ($B220^{+}CD21^{lo}CD23^{+}$); MzB, marginal zone B cells ($B220^{+}CD21^{hi}CD23^{-}$); TrB, transitional B cells ($B220^{+}CD21^{lo/-}CD23^{-}$); $CD4^{+}$ and $CD8^{+}$ T cells. Relative copy number (RCN) of murine *Cd300lb* and *TLR4* after normalization with *GAPDH*. The graph in (A) shows mean values + SD from two experiments.
(B) Flow cytometry analysis of CD300b and TLR4 expression on *WT* and *Cd300lb*$^{-/-}$ Macs differentiated from the bone marrow or isolated from the peritoneal cavities or organ tissues. The dot plots shown in (B) are representative of three experiments.

(C) F4/80 staining of macrophages in the lung tissues from PBS- or Cl_2MBP-treated *WT* and *Cd300lb*$^{-/-}$ mice. Arrows indicate positive staining of macrophages. Tissue sections shown are representative of 5 mice per group.
(D-F) Numbers of macrophages, DCs and neutrophils were determined by flow cytometry and normalized according to the volume (peritoneal cavity, D) or the weight of lung (E) or spleen (F) tissue.
(G) Anti(α)-Ly6G- or αIgG Ab-treated *WT* and *Cd300lb*$^{-/-}$ mice (n = 6) were i.p. injected with a toxic dose of LPS (37 mg/kg). Mouse survival was monitored every 6 h for 7 days.
(H) Cytokine concentrations from sera from αLy6G- or αIgG Ab-treated *WT* and *Cd300lb*$^{-/-}$ mice were determined by flow cytometry at 2 h post LPS treatment.
(I) αNK1.1- or αIgG Ab-treated *WT* and *Cd300lb*$^{-/-}$ mice (n = 6) were i.p. injected with a toxic dose of LPS (37 mg/kg). Mouse survival was monitored every 6 h for 7 days.
(J) Cytokine concentrations from sera from αNK1.1- or αIgG Ab-treated *WT* and *Cd300lb*$^{-/-}$ mice were determined by flow cytometry at 2 h post LPS treatment. The graphs in (D-F, H and J) show mean values + SEM from 5 mice per group; NS, not significant; *p≤0.05, **p≤0.01, and ***p≤0.001.

Figure S4, related to Figure 5 and 6. Recognition of LPS by CD300b-TLR4 co-expression macrophages but not dendritic cells modulates TLR4-mediated cytokine responses in a CD300b and CD14 dependent manner.
(A) Flow cytometry analysis of CD300b and TLR4 expression on *WT* macrophages (Macs) or dendritic cells (DCs) differentiated from either the bone marrow or isolated from the peritoneal cavity.
(B) Bone marrow-derived DCs from *WT* or *Cd300lb*$^{-/-}$ mice and stimulated with 2 μg/ml of LPS for various lengths of time. Cytokine levels were assessed by flow cytometry.
(C) Co-localization of CD300b and TLR4 on bone marrow-derived macrophages from *WT*, *Cd300lb*$^{-/-}$ or *TLR4*$^{-/-}$ mice, receiving no treatment (NT) or following LPS treatment (2 μg/ml, 0.2 h). Potential cross-reactivity was validated using isotype-specific αIgG Ab stainings.
(D) The graph shows the quantification of CD300b co-localization with TLR4, as determined in (C).
(E-F) Bone marrow-derived macrophages (BMMs) from *WT* or *Cd300lb*$^{-/-}$ mice were pretreated for 12 h with αIgG isotype control Ab, αCD300b Ab, αCD14 Ab, or both αCD300b and αCD14 Abs before the addition of 10 μg/ml FITC-labeled LPS for 2 h at 37°C (E) or 4°C (F). Binding was analyzed by flow cytometry and displayed as MFI.
(G-H) BMMs from *WT*, *Cd300lb*$^{-/-}$ or *Cd14*$^{-/-}$ mice were incubated with 10 μg/ml FITC-labeled LPS from *E. coli* (G) or *S. minnesota* (H) for 0.5 h at 4°C. Binding was analyzed by flow cytometry and displayed as percentage of LPS binding after considering LPS-binding from *WT* BMMϕ as 100%.
(I) Levels of cytokine secreted from *WT* or *Cd300lb*$^{-/-}$ BMMs treated with Abs and LPS as described in (E). Histograms shown in (A) and co-localization data in (C) are representative of three experiments. The error bars in graphs (B, D-I) show mean values SEM; NS, not significant; *p≤0.05, **p≤0.01 and ***p≤0.001.

Figure S5, related to Figure 6. Recognition of LPS by CD300b-expressing macrophages regulates efferocytosis and TLR4-MyD88- and TLR4-TRIF-dependent inflammatory cytokine responses.
(A-C) BMMs from *WT* mice were co-cultured with pHrodo-labeled apoptotic cells (AC) at a ratio of 1:2 (BMMs:AC) in presence or absence of LPS (2 μg/ml) for various lengths of time.
(A) Samples were collected after 12 h, lysed and then immunoprecipitated with an anti-CD300b or anti-IgG isotype control Ab. After SDS-PAGE and transfer to nitrocellulose membranes, samples were detected by immunoblotting with the indicated Abs.
(B) Samples were analyzed for engulfment of AC by flow cytometry.
(C) Cell culture supernatants were analyzed for TNFα and IL-10 production after 2 and 12 h incubation by flow cytometry.
(D-G) BMMs from *WT* or *Cd300lb*$^{-/-}$ mice were treated with the diluent control DMSO (D), the Syk inhibitor, Piceantannol (Pic, 10 μM), or the PI3K inhibitor, Wortmannin (Wo, 10 μM), for 1 h prior to stimulation with 2 μg/ml of LPS for additional 2 h.
(D) IL-10 cytokine levels in the culture medium from *WT* or *Cd300lb*$^{-/-}$ BMMs-treated with D, Wo, or Pic were determined by flow cytometry.
(E) AKT and ERK1/2 phosphorylation level was analyzed by immunoblotting with the indicated Abs.
(F-G) D-, Wo-, or Pic-treated BMMs from *WT* or *Cd300lb*$^{-/-}$ mice were stimulated with 2 μg/ml of LPS, and cell lysates were immunoprecipitated with anti-TLR4 or anti-IgG isotype control Ab. Samples were

analyzed by immunoblotting with the indicated Abs while association pattern was quantified by densitometry and expressed as fold increase after considering binding intensity from NT-*WT* BMMs as baseline binding.
(H) BMMs from *WT* or *Cd300lb*$^{-/-}$ mice were treated with the ERK1/2 inhibitor PD98059 (25 μM) for 1 h prior to stimulation with 2 μg/ml of LPS for additional 2 h. Levels of pro-inflammatory cytokines in the culture medium were determined by flow cytometry.
(I) IFN-β cytokine level in the culture medium from LPS-treated *WT* or *Cd300lb*$^{-/-}$ BMMs was determined by flow cytometry.
(J) BMMs from *WT*, or *Cd300lb*$^{-/-}$ mice were stimulated with 2 μg/ml of LPS for various lengths of time and cell lysates were analyzed for the levels of phosphorylated or total protein expression by immunoblotting with the indicated Abs. Data shown in (A, E, F and J) are a representative of three experiments. Error bars in graphs (B-D and G-I) show mean values SEM; NS, not significant; *p≤0.05, **p≤0.01 and ***p≤0.001.

Figure S6, related to Figures 1-6. Model of CD300b function
CD300b is a PS-receptor that under physiological conditions regulates efferocytosis in a DAP12-dependent manner (Murakami et al., 2014), thus maintaining cellular homeostasis (*left*). Upon acute bacterial infection, CD300b binds LPS, and forms a complex with TLR4-CD14. CD300b-dependent recruitment of DAP12, Syk and PI3K promotes the formation of a CD300b-DAP12-TLR4-Syk-PI3K signaling complex. This results in the PI3K-mediated phosphorylation of AKT and, likely, in alteration of PtdIns(4,5)P_2 levels through PtdIns(3,4,5)P_3 synthesis (Kagan and Medzhitov, 2006; Patel and Mohan, 2005) that could facilitate the dissociation of MyD88-TIRAP from the complex, leading to a reduced activation of the MEK1/2-ERK1/2-NFκB signaling cascade and lower IL-10 production. Moreover, CD300b plays a role in TLR4-CD14-TRIF signaling by increasing the IFN-β response. Since TRIF signaling originates subsequent to endocytosis and DAP12 facilitates TLR4 endocytosis and TRIF signaling (Zanoni et al., 2011), CD300b likely also regulates endocytic signaling of the TLR4 complex (through DAP12 recruitment). Thus, CD300b links TLR4-CD14-TRIF-IRF3 signaling and the DAP12-Syk-PI3K cascade. Overall, this results in elevated pro-inflammatory cytokine production leading to recruitment of inflammatory cells, which during a prolonged exposure to LPS (i.e. lethal endotoxemia and septic peritonitis) turns into uncontrolled amplification of inflammation. We predict that the level of CD300b-mediated DAP12 recruitment to the TLR4-MyD88 and TLR4-CD14-TRIF signaling complexes is dependent on the severity of infection thereby effecting the balance between pro- and anti-inflammatory cytokines produced by these two pathways (*middle*). In the case of CD300b-deficiency, DAP12, Syk, and PI3K are not recruited to the TLR4 complex, resulting in sustained association of MyD88-TIRAP, which leads to an elevated ERK1/2 activation, prolonged activation of NFκB and presumably AP-1, thereby promoting an enhanced IL-10 response. In addition, the lack of DAP12 recruitment likely affects TLR4 internalization, resulting in a reduced activation of TRIF-IRF3 pathway. Consequently, the reduced pro-inflammatory cytokine response and elevated IL-10 levels allow for the subsequent survival from an acute infection, and excessive LPS exposure (*right*). Dashed grey lines indicate dampened/inhibited signaling, solid black lines indicate activated signaling, and question marks indicate putative processes or pathways.

Supplementary Experimental Procedures:

Animals
Heterozygous *Cd3000lb*$^{+/-}$ male and female littermates were kindly provide by Dr. Jiro Kitaura (University of Tokyo, Japan) and were described previously (Yamanishi et al., 2012). All experiments were conducted using female *Cd300lb*$^{-/-}$, *Cd300lb*$^{-/-}$ *IL-10*$^{-/-}$ and *Cd300lf*$^{-/-}$ C57BL/6 mice and their corresponding *WT* littermates, as described elsewhere (Yamanishi et al., 2012; Tian et al., 2014). *IL-10*$^{-/-}$ C57BL/6 mice were kindly supplied by Ms. Robin Winkler-Pickett (Cancer and Inflammation Program, National Cancer Institute, MD, USA). Femurs and tibias of *TLR4*$^{-/-}$ mice were kindly provided by Dr. Stefanie N. Vogel (University of Maryland, MD, USA), while *Cd14*$^{-/-}$ BMMs were a gift from Dr. Jonathan C. Kagan (Harvard Medical School, MA, USA). All animals were bred and housed in a pathogen-free environment in the NIAID animal facility with experimental protocols (LIG5E) approved by the NIAID Animal Care and Use Committee.

Antibodies and reagents

Anti-CD300b monoclonal (MAB2580) or polyclonal (AF2580) Abs and isotype control goat IgG Ab were from R&D, and were labeled with Alexa488 using the Alexa488 antibody labeling kit (Invitrogen), according to the manufacturer's instructions. Syk (D3Z1E), pPI3K (#4228), PI3K (6G10), pAkt (D9E), Akt (#9272), pERK1/2 (3A7), ERK1/2 (#9102), pMEK1/2 (41G9), MEK1/2 (#9122), pJNK (G9), JNK (#9251), TIRAP (D6M9Z), pNFκB (93H1), NFκB (D14E12), pp38 (D3F9), p38 (D13E1), pTBK1 (D52C2), TBK1 (D1B4), pIKKε (D1B7), IKKε (#2690), pIRF3 (4D4G), IRF3 (D83B9) Abs were from Cell Signaling Technology. GAPDH (FL-355), DAP12 (FL-113), TLR4 (25), and MyD88 (HFL-296) Abs, and HRP-conjugated secondary Abs (anti-mouse, anti-rabbit, anti-rat, and anti-goat) were from Santa Cruz Biotechnology. The Alexa647 antibody labeling kit and the pSyk (F.724.5) and TLR4 (76B357.1) Abs were from Thermo Scientific. Anti-CD14 (4C1) was from BD Biosciences and anti-human IgG-Fcγ fragment specific Ab was from Jackson ImmunoResearch. The PI3K inhibitor, Wortmannin, the Syk inhibitor, Piceantannol, p38 inhibitor, SB203580, and the ERK1/2 inhibitor, PD98059, were obtained from Calbiochem, and dissolved in the diluent dimethyl sulfoxide (DMSO, Sigma). Rhodamine-conjugated TLR2-TLR1 (PAM3CSK4)-, TLR3 (Poly(I:C))-, NOD2 (MDP)-specific ligands were from InvivoGen, and FITC-conjugated TLR4 (LPS) ligand or FITC-conjugated *E. coli* were obtained from Invitrogen. LPS-*E.coli* (0127:B8) was obtained from Sigma. LPS-*E.coli* (0111:B4), LPS-*E.coli* (055:B5), LPS-*E.coli* (EH100 (Ra), LPS-*E.coli* (R515 (Re), Lipid A-*E.coli* (R515 (Re) and purified mTLR4-hFc were purchased from Enzo Life Sciences. Recombinant mCD14 was obtained from Sino Biological Inc., mLAIR1 was purchased from R&D.

DNA reagents.

The generation of the pCDH-EF1-T2A-puro (pCDH) vector (System Biosciences) lentivirus expression constructs carrying mCD300b, mCD300f, FcRγ, or DAP12 genes were previously described (Tian et al., 2014; Murakami et al., 2014; Yamanishi et al., 2012). The constructs for the IgG-Fc portion fused to hCD300b (hCD300b-Fcγ), mCD300b (mCD300b-Fcγ), mCD300d (mCD300d-Fcγ), mCD300f (mCD300f-Fcγ) or the control protein, NITR (NITR-Fcγ), extracellular domains in a pcDNA backbone were kindly supplied by Dr. John P. Cannon (Cannon et al., 2011).

Cell culture, transfection and infection

L929 and HEK293T cells were cultured in DMEM medium with 10% FBS. HEK293T cells were transfected using PolyJet (Signagen). Lentivirus particles were generated by co-transfection of HEK293T cells with pCDH-puro vector encoding mCD300b, mCD300d, mCD300f, mFcRγ, mDAP12, or psPAX2, and pMD2G helper plasmids. L929 cells were infected with lentivirus particles for 24 h at 37°C, in the presence of 6 μg/ml protamine sulfate. Selection with 20 μg/ml puromycin started 48 h after infection and clonal cell lines were obtained using the limiting dilution method as previously described (Murakami et al., 2014).

Chimeric proteins

HEK293T cells were transiently transfected with pcDNA3.0 plasmids encoding hCD300b-Fcγ, mCD300b-Fcγ, mCD300d-Fcγ, mCD300f-Fcγ or NITR-Fcγ constructs using PolyJet, and chimeric proteins were purified as previously described (Murakami et al., 2014).

Protein induction and purification

The Ig-domain of mCD300b was PCR-amplified from the pCDNA3-mCD300b-Fcγ plasmid (Cannon et al., 2011), using primers 5'-CACCCATATGCAAGGCCCAGCATTGGTGAGG-3' and 5'-GCGGCCGCTTAGTAGACGTTCACTTTAAC-3' and cloned into pET21b using the restriction enzyme sites *Nde*I and *Not*I. The Ig-domain of mCD300b was expressed as described previously (Sgourakis et al., 2015). Briefly, CD300b-Ig-domain was expressed in Rosetta 2 (DE3) *E.coli* using 1 mM IPTG (isopropyl 1-thio-β-D-galactopyranoside) as inclusion bodies. Following washing in Tris/EDTA and solubilization in 6 M guanidine HCl, the protein was refolded by dilution into refolding buffer (0.4 M arginine HCl, 0.1 M Tris, pH 8, 2 mM EDTA, 5 mM reduced glutathione, 0.5 mM oxidized glutathione) for 7 days at 4°C; dialyzed against 150 mM NaCl and 25 mM MES, pH 6.5; concentrated with an Amicon stirred cell concentrator using an Ultracell 10-kDa ultrafiltration regenerated cellulose filter (Millipore);

purified by gel filtration on Superdex HR 75 followed by ion exchange chromatography and maintained in PBS at 4°C.

Surface plasmon resonance (SPR)

The interaction of Fcγ-chimeric or monomeric proteins with LPS was measured using the BIAcore T100 SPR instrument (GE Healthcare) at 25°C as previously described (Murakami et al., 2014). For LPS and protein interactions, 1 μM biotinylated LPS (*E. coli*, serotype 0111:B4, InvivoGen) was captured on an S Sensor Chip SA (GE Healthcare). The remaining binding sites on the chips were blocked using 50 μM Amino-PEO-biotin. The interaction with LPS was assessed by injection with various concentrations of hCD300b-Fcγ, mCD300b-Fcγ, mCD300a-Fcγ, mCD300d-Fcγ, mCD300f-Fcγ, NITR-Fcγ, or mCD300b, mCD14 and mLAIR1 proteins, ranging from 0.125 to 5 μM. Dissociation constants (K_D) were calculated using BIAevaluation software as described previously (Sgourakis et al., 2015). For LPS blocking experiments, purified mCD300b (0.5 μM) was pre-incubated for 0.5 h at 4°C with different concentrations of wild-type LPS: LPS-*E.coli* (0111:B4), LPS-*E.coli* (0127:B8), LPS-*E.coli* (055:B5) or structural components of LPS: lipid A-*E.coli* (R515 (Re), LPS-*E.coli* (EH100 (Ra), and LPS-*E.coli* (R515 (Re), ranging from 1-100 μg/ml. Binding data were acquired with a flow rate of 20 μl/min for 2 min. After 2 min dissociation, the bound analytes were removed by a 1 min regeneration phase with a washing buffer containing 2.5 M NaCl and 50 mM NaOH.

Cell based TLR-ligand binding assays

Rhodamine-labeled TLR2-TLR1 (PAM3CSK4)-, TLR3 (Poly(I:C))-, NOD2 (MDP)-specific ligands or FITC-labeled TLR4 (LPS)-ligand purified from either *E. coli* or *S. minnesota* (10 μg/ml) were incubated with mCD300b-DAP12-, mCD300d-FcRγ-, mCD300f-, EV-expressing L929 cells or BMM from *WT*, *Cd300lb*$^{-/-}$, *and Cd14*$^{-/-}$ mice, then incubated for up to 2 h at 37°C or 4°C. Binding was determined by flow cytometry and represented as mean fluorescence intensity (MFI) or percentage of LPS binding.

Cecal Ligation Puncture (CLP) and lethal endotoxemia

CLP was performed as described previously (Leelahavanichkul et al., 2014). Briefly, the cecum was ligated and punctured twice with a 21-gauge needle, then gently squeezed to express a small amount of fecal material, and returned to the central abdominal cavity. Sham-control mice were subjected to a similar laparotomy without ligation and puncture. Pre-warmed normal saline (40 ml/kg) was immediately given intraperitoneally (i.p.) after surgery and slow release buprenorphrine (0.5 mg/kg) was given subcutaneously every 72 h for pain management. Lethal endotoxemia was induced by i.p. injection of LPS (37 mg/kg, *E.coli,* serotype 0127:B8), dissolved in 0.1 ml PBS. At 2, 6 and 12 h after CLP surgery or LPS-induced lethal endotoxemia, blood was collected and serum cytokine levels were measured by flow cytometry. Lung tissue specimens were collected after 12 h and fixed in 10% neutral-buffered formalin for histology.

Measurement of cytokines and chemokines

TNFα, IFNγ, IL-6, IL-10, IL-12, and MCP-1 concentrations were measured using the Cytometric Bead Array (CBA) mouse inflammatory kit (BD Biosciences), while IFN-β levels were assessed using the LEGENDplex mouse inflammation kit (BioLegend) following the manufacturer's instructions.

Histological analysis

All tissue samples were fixed in 10% formalin and tissue sections were stained with hematoxylin and eosin (H&E) or anti-F4/80 Ab (eBiosciences, BM8). F4/80 immunostaining was performed using the LeicaBiosystems Intense R Detection Kit following the manufacture's recommendations as previously described (Qi et al., 2000). Stained sections were scanned by a ScanScope XT (Aperio Technologies) and analyzed using Aperio Image Scope software (version 11).

Assessment of bacterial burden in fluids and organs of septic mice

Bacterial colony-forming units in blood, peritoneal cavity, lung, spleen and liver were assessed in CLP-treated *WT* and *Cd300lb*$^{-/-}$ mice. Bacterial burden was determined 24 h after CLP-treatment. The number of colony formation units (c.f.u.) was determined by plating 10-fold serial dilutions of blood. For assessing the bacterial load in organ tissues, equal amount (g) of tissue was homogenized and 10-fold serial dilutions were plated. A 100 μl aliquot of each dilution was spread on brain heart infusion agar plates without

antibiotics and incubated under aerobic conditions at 37°C for 24 h.

Depletion of neutrophils and NK cells

For *in vivo* depletion of neutrophils, mice were injected i.p. with 500 μg anti-Ly6G (clone 1A8, BioxCell) or control Ab (clone 2A3, BioxCell) 24 h before the induction of lethal endotoxemia. For depletion of NK cells, mice were injected i.v. with 500 μg anti-NK1.1 (clone PK136, BioxCell) or control Ab (clone C1.18.4, BioxCell) at 5, 3 and 1 day before the induction of lethal endotoxemia.

Extract preparation, immunoprecipitation and western blot analysis

BMM were lysed for 1 h at 4°C in ice-cold lysis buffer A [20 mM Tris, pH 7.4, 137 mM NaCl, 10% glycerol, 1% NP40, supplemented with protease and phosphatase inhibitory cocktails (Sigma)]. Cellular debris was removed by centrifugation at 10,000 x g for 15 min at 4°C. Equal amounts of protein, as determined by Bradford assay, were loaded for SDS-PAGE, then transferred onto nitrocellulose membranes. Membranes were probed with Abs of interest, followed by enhanced chemiluminescence with secondary Abs conjugated to horseradish peroxidase.

For immunoprecipitation experiments, 2 mg of each lysate was immunoprecipitated overnight at 4°C with anti-CD300b Ab, anti-TLR4 Ab or IgG isotype as control, followed by 12 h incubation with 10 μl of protein G-agarose dynabeads (Invitrogen). Immunoprecipitates were washed three times with lysis buffer A and reactions were analyzed by immunoblotting. For cross-linking of cells followed by immunoprecipitation experiments, BMM were incubated with 2.5 mM of DSP for 20 min at RT and reactions were quenched using 0.5 M Tris, pH 7.5 for additional 15 min (Ahn et al., 1999; Shenoy et al., 2006; Corgiat et al., 2013). Samples were lysed for 1 h at 4°C in ice-cold lysis buffer B [50 mM Hepes, pH 7.5, 150 mM NaCl, 10% glycerol, 1% NP40, supplemented with protease and phosphatase inhibitory cocktails]. Two mg of each lysate was incubated with 20 μl of anti-CD300b or IgG isotype Ab coupled to protein A-Sepharose (50% slurry) for additional 2 h at 4°C. Immunoprecipitates were washed and analyzed by immunoblotting.

For cross-linking experiments of recombinant proteins, mCD300b, mCD14 and mTLR4 proteins were mixed using equal molar ratios (1:1:1) in the presence or absence of 2 μg/ml LPS for 1 h at 4°C. Reactions were incubated with 2.5 mM of dithiobissuccinimidyl propionate (DSP) for 10 min at RT and the reaction was quenched using 0.5 M Tris, pH 7.5 for additional 15 min. Samples were incubated with 10 μl of anti-CD300b or IgG isotype Ab coupled to protein A-Sepharose (50% slurry) for additional 2 h at 4°C. Immunoprecipitates were washed and analyzed by immunoblotting.

LPS binding to mCD300b-, mCD300d-, mCD300f-, or NITR-Fcγ chimeric proteins was determined using a streptavidin pulldown assay. Biotin-conjugated LPS (InvivoGen) was mixed with different concentrations of Fcγ-chimeric proteins. Reactions were incubated overnight at 4°C in lysis buffer C (20 mM Tris, pH 7.4, 137 mM NaCl, 10% glycerol, 0.5% NP40), followed by 1 h incubation with 5 μl of streptavidin-magnetic beads (New England BioLabs). Beads were washed 3 x with lysis buffer C and reactions were analyzed by immunoblotting using an anti-human IgG-Fcγ-specific Ab.

Competition assays

For competition experiments, FITC-labeled LPS-*E. coli* (10 μg/ml) was incubated with mCD300b-DAP12-expressing L929 cells at 4°C in the presence of increasing concentrations of unlabeled LPS from either *E. coli, or S. minnesota*, ranging from 1 to 100 μg/ml. Zymosan A (a TLR2-ligand) was used as control. Samples were analyzed by flow cytometry and MFI values from reactions without unlabeled LPS were considered as the maximum binding level (0% Inhibition).

For Ab blocking experiments, BMM from *WT* or *Cd300lb*$^{-/-}$ mice were pretreated for 12 h with anti-IgG isotype control Ab (5 μg), anti-CD300b Ab (5 μg), anti-CD14 Ab (5 μg) or both anti-CD300b Ab (2.5 μg), anti-CD14 Ab (2.5 μg) before the addition of 10 μg/ml FITC-labeled LPS for 2 h at 37°C or 4°C. Binding was analyzed by flow cytometry.

Confocal microscopy

BMM from *WT*, *Cd300lb*$^{-/-}$, *and TLR4*$^{-/-}$ mice were plated for 12 h prior on number 1.5 glass dishes (MatTek Corporation). Then, cells were either treated with LPS (2 μg/ml) for 20 min at 37°C or left unstimulated (NT), followed by staining with Alexa647-conjugated anti-TLR4 Ab or an anti-IgG isotype control Ab for 2 h at 4°C. Next, cells were washed twice with PBS and fixed with methanol:acetic acid

(95%:5%) for 10 min at -20°C. Cells were then blocked with 10% BSA in PBS, followed by incubation with an Alexa488-conjugated anti-CD300b or anti-IgG isotype control Ab for 2 h at 4°C. Cells were washed twice with PBS, mounted in ProLong Gold medium (Invitrogen) and visualized by a LSM 780 laser scanning confocal microscope (Zeiss) with a 63 x Zeiss Plan-Apochromat objective. Co-localization was assessed by analysis of overlapping pixels occupied by two fluorophores, using Imaris software and its co-localization function (v. 7.6; Bitplane), as described previously (Krzewski et al., 2013).

Flow cytometry

To assess CD300b and TLR4 expression profiles on macrophages (Mac) from the bone marrow, peritoneal cavity, lung or spleen, cells were stained with Alexa488-conjugated anti-CD300b and APC-conjugated anti-TLR4 Abs. The expression of CD300b and TLR4 was determined on Mac ($F4/80^{+}$, $CD11b^{hi}$, $CD11c^{-}$ $Ly6G^{-}SSC^{lo}$) by using cell type specific Abs, as indicated in the text.

For cell sorting experiments, lung or splenic cells were first isolated by homogenization and then passed through nylon mesh strainers (70 μm, Fisher Scientific). Cells were treated with an anti-CD16/32 Ab (2.4G2, BD Biosciences) to block Fc receptor binding, and then stained with the indicated Abs in PBS containing 0.2% FBS. All Abs were obtained from BioLegend and included the following molecules: CD16/CD32 (93), CD3 (145-2C11), CD4 (RM4-5), CD8 (53-6.7), CD11b (M1/70), CD11c (N418), CD19 (MB19-1), CD21 (eBio8D9), CD23 (B3B4), B220 (RA3-6B2), NK1.1 (PK136), PDCA-1 (eBio927), F4/80 (BM8), TLR4 (SA15-21), and Ly6G (1A8). Dead cells were excluded using Zombie NIR™ (BioLegend) staining following the manufactures recommendations. Stained cells were sorted with a FACS Aria-Red (BD Bioscience) and analyzed with FlowJo software (v.10, Tree Star).

Differentiation of bone marrow-derived macrophages and DC

Bone marrow cells were isolated from femurs and tibias of *WT*, *Cd300lb*$^{-/-}$, *Cd300lb*$^{-/-}$ *IL-10*$^{-/-}$, *Cd300f*$^{-/-}$ or *TLR4*$^{-/-}$ mice. Differentiation of BMM was induced by culturing bone marrow cells in RPMI 1640 medium supplemented with 10% FBS and 30% L929-conditioned medium (a source of macrophage colony-stimulating factor), while differentiation of DC was induced by culturing cells in RPMI 1640 medium supplemented with 10% FBS and 20 ng/ml granulocyte-macrophage colony-stimulating factor (GM-CSF). BMM or DC were cultured for 7 days with one renewal of the culture medium.

Phagocytosis of apoptotic cells

Thymocytes from C57BL/6 mice were incubated with 10 μM dexamethasone in RPMI medium with 1% FBS for 6 h for the generation of apoptotic cells (AC) (Tian et al., 2014; Yamanishi et al., 2012). The AC were labeled with pHrodo succinimidyl ester (Invitrogen) according to the manufacturer's instruction. BMMϕ (2×10^{5}) were incubated with pHrodo-labeled AC at a ratio of 1:2 for various lengths of time at 37°C and stained using an anti-mouse F4/80 Ab. Cells were washed and suspended in basic buffer (pH 8.8) to quench the fluorescence of non-engulfed pHrodo-labeled AC before the flow cytometry analysis.

RNA isolation and quantitative real-time RT-PCR

Total RNA was isolated using the RNAquous-4PCR kit (Ambion) following the manufacturer's instructions. cDNA was synthesized with Qscript cDNA synthesis kits (Quanta Biosciences) and quantitative real-time PCR (qRT-PCR) was performed as previously described (Murakami et al., 2014). Oligonucleotide primers for amplifying *murine Cd300lb*, *TLR4* and *GAPDH* were purchased from Qiagen. Relative copy number (RCN) of murine *Cd300lb* and *TLR4* were normalized by the expression of the housekeeping gene, *GAPDH*, and calculated with the equation: $RCN = E^{-\Delta Ct}$, where E = efficiency of PCR, and Ct = Ct *target* − Ct *GAPDH*. Melting curve analyses were performed at the end of each run to ensure that only one product was amplified.

Supplementary References:

Cannon, J.P., O'Driscoll, M., and Litman, G.W. (2011). Specific lipid recognition is a general feature of CD300 and TREM molecules. Immunogenetics *64*, 39-47.

Ahn, S., Maudsley, S., Luttrell, L.M., Lefkowitz, R.J., and Daaka, Y. (1999). Src-mediated Tyrosine Phosphorylation of Dynamin Is Required for β2-Adrenergic Receptor Internalization and Mitogen-

activated Protein Kinase Signaling. J Biol Chem *274*, 1185-1188.

Corgiat, B.A., Nordman, J.C., and Kabbani, N. (2013). Chemical crosslinkers enhance detection of receptor interactomes. Front Pharmacol *4*, 1-6.

Krzewski, K., Gil-Krzewska, A., Nguyen, V., Peruzzi, G., and Coligan J.E. (2013). LAMP1/CD107a is required for efficient perforin delivery to lytic granules and NK cell cytotoxicity. Blood *121*, 4672-4683.

Leelahavanichkul, A., Souza, A.C., Street, J.M., Hsu, V., Tsuji, T., Doi, K., Li, L., Hu, X., Zhou, H., Kumar, P.*, et al.* (2014). Comparison of serum creatinine and serum cystatin C as biomarkers to detect sepsis-induced acute kidney injury and to predict mortality in CD-1 mice. Am J Physiol Renal Physiol *307*, F939-948.

Patel, R.K., and Mohan, C. (2005). PI3K/AKT signaling and systemic autoimmunity. Immunol Res *31*, 47-55.

Qi, C.F., Hori, M., Coleman, A.E., Torrey, T.A., Taddesse-Heath, L., Ye, B.H., Chattopadhyay, S.K., Hartley, J.W., and Morse, H.C., III. (2000). Genomic organization and expression of BCL6 in murine B-cell lymphomas. Leuk Res *24*, 719-732.

Sgourakis, N.G., May, N.A., Boyd, L.F., Ying, J., Bax, A., and Margulies, D.H. (2015). A novel MHC-I surface targeted for binding by the MCMV m06 Immunoevasin revealed by solution NMR. J Biol Chem *290*, 28857-28867.

Shenoy, S.K., Drake, M.T., Nelson, C.D., Houtz, D.A., Xiao, K., Madabushi, S., Reiter, E., Premont, R.T., Lichtarge, O., and Lefkowitz, R.J. (2006). β-Arrestin-dependent, G Protein-independent ERK1/2 activation by the β2-adrenergic receptor. J Biol Chem *274*, 1261-1273.